



# Estimation of local anisotropy of plexiform bone: Comparison between depth sensing micro-indentation and Reference Point Indentation



E. Dall'Ara<sup>a,b,c,\*</sup>, P. Grabowski<sup>c</sup>, P. Zioupos<sup>d</sup>, M. Viceconti<sup>a,b</sup>

<sup>a</sup> Department of Mechanical Engineering, University of Sheffield, Sheffield, UK

<sup>b</sup> INSIGNEO Institute for in silico medicine, University of Sheffield, Sheffield, UK

<sup>c</sup> Department Oncology and Metabolism, University of Sheffield, Sheffield, UK

<sup>d</sup> Centre for Musculoskeletal & Medicolegal Research, CFI, Cranfield University, DA of the UK, Shrivernham, UK

## ARTICLE INFO

### Article history:

Accepted 1 October 2015

### Keywords:

Bone  
Reference Point Indentation  
Micro-indentation  
Anisotropy  
Plexiform

## ABSTRACT

The recently developed Reference Point Indentation (RPI) allows the measurements of bone properties at the tissue level *in vivo*. The goal of this study was to compare the local anisotropic behaviour of bovine plexiform bone measured with depth sensing micro-indentation tests and with RPI. Fifteen plexiform bone specimens were extracted from a bovine femur and polished down to 0.05  $\mu\text{m}$  alumina paste for indentations along the axial, radial and circumferential directions ( $N=5$  per group). Twenty-four micro-indentations (2.5  $\mu\text{m}$  in depth, 10% of them were excluded for testing problems) and four RPI-indentations ( $\sim 50 \mu\text{m}$  in depth) were performed on each sample. The local indentation modulus  $E_{\text{ind}}$  was found to be highest for the axial direction ( $24.3 \pm 2.5$  GPa) compared to the one for the circumferential indentations (19% less stiff) and for the radial direction (30% less stiff). RPI measurements were also found to be dependent on indentation direction ( $p < 0.001$ ) with the exception of the Indentation Distance Increase (IDI) ( $p=0.173$ ). In particular, the unloading slope US1 followed similar trends compared to the  $E_{\text{ind}}$ :  $0.47 \pm 0.03$  N/ $\mu\text{m}$  for axial, 11% lower for circumferential and 17% lower for radial. Significant correlations were found between US1 and  $E_{\text{ind}}$  ( $p=0.001$ ;  $R^2=0.58$ ), while no significant relationship was found between IDI and any of the micro-indentation measurements ( $p > 0.157$ ). In conclusion some of the RPI measurements can provide information about local anisotropy but IDI cannot. Moreover, there is a linear relationship between most local mechanical properties measured with RPI and with micro-indentations, but IDI does not correlate with any micro-indentation measurements.

© 2015 The Authors. Published by Elsevier Ltd. This is an open access article under the CC BY license (<http://creativecommons.org/licenses/by/4.0/>).

## 1. Introduction

Bone is a complex hierarchical material with mechanical properties that depend on the investigated dimensional scale, from the cell up to the body levels. Bone structural units (BSU) are formed of packages of bone lamellae that organize in macrostructures such as trabeculae and osteons. Due to the distribution of their BSUs, both cortical and trabecular bone have exhibited anisotropic mechanical properties at the tissue level as shown by micro-indentation (Dall'Ara et al., 2013; Franzoso and Zysset, 2009; Reisinger et al., 2011; Roy et al., 1999; Wolfram et al., 2010) and ultrasound (Turner et al., 1995, 1999); and at the macro-level as shown by mechanical testing (Li et al., 2013; Odgaard, 1997; Ohman et al., 2007; Rincon-Kohli and

Zysset, 2009). The long bones of quickly growing large animals reveal one further sub-classification into laminar and plexiform tissue, formed of parallel-fibred bone and lamellar bone around macroporosities. Previous studies have shown that the structure of plexiform bone has an orthotropic mechanical behaviour macroscopically (Katz et al., 1984; Macione et al., 2010). However, not much is known about its mechanical anisotropy at the BSU level. The better understanding of the anisotropic properties of this structure at the micro-level is important in order to understand why it appears only in large quickly growing animals and not in more active species such as humans or small mammals.

The need to understand how bone properties relate and translate from the micro-architectural (BSU) to the macro-architectural level has become more acute with arrival of the Reference Point Indentation (RPI) method. This novel indentation technique allows for the study of bone quality *in vivo* (Hansma et al., 2008, 2009), something that until now could be done only on extracted bone biopsies. A few studies have reported that some of the RPI parameters, in particular the Indentation Distance Increase IDI (Diez-Perez et al., 2010; Guerri-

\* Correspondence to: INSIGNEO Institute for in silico medicine, Room C+36-C+ Floor, The Pam Liversidge Building, Sir Frederick Mappin Building, Mappin Street, Sheffield S1 3JD, UK.

Tel.: +44 114 2226175; fax: +44 114 2227890.

E-mail address: [e.dallara@sheffield.ac.uk](mailto:e.dallara@sheffield.ac.uk) (E. Dall'Ara).

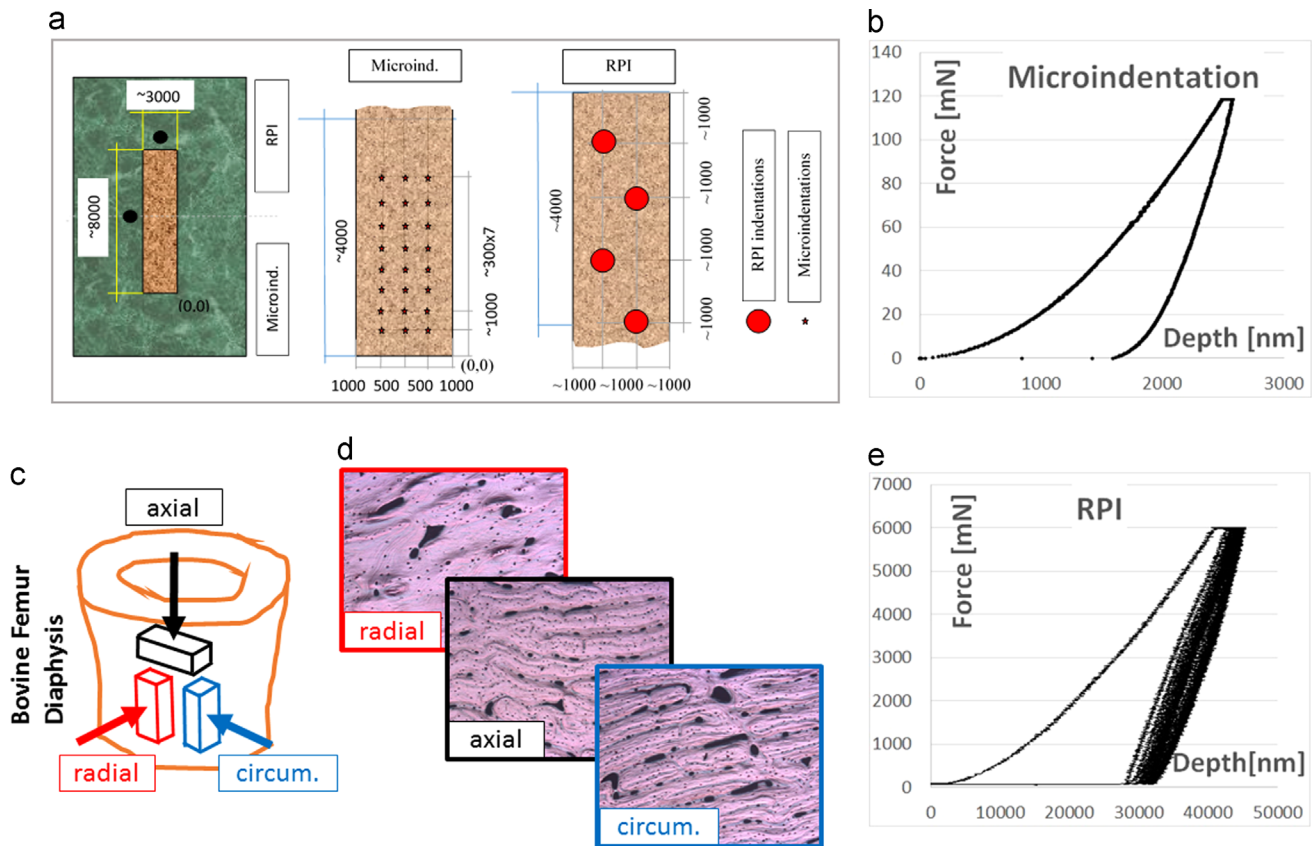


**Fig. 1.** Overview of the methods. Specimens were extracted from a bovine femur in order to perform indentations along axial, circumferential and radial directions (c). Only specimens with plexiform structure were analyzed (d). Specimens were embedded in PMMA and indented thirty times with micro-indentation test (a, b) and four times with Reference Point Indentation (RPI) test (a, e).

Fernandez et al., 2013), differ between patients who did or did not suffer of a bone fracture. However, it is not clear yet how the properties measured with this tool are related to the intrinsic mechanical properties of the tested bones at the tissue level and to its structural anisotropy. Very recently some methodological studies investigated the sensitivity of the RPI indentation properties to the selected testing procedure *in vitro* (Jenkins et al., 2015; Setters and Jasiuk, 2014). Due to the relatively large indentations (50–200  $\mu\text{m}$  in depth) and the potential relationship between the local resistance to fracture and the IDI, some other studies have compared the RPI outputs with measurements performed at the macro-level such as bone toughness and reported mixed if not controversial results. In particular, IDI was not related to the whole mouse bone stress intensity fracture toughness (Carriero et al., 2014), was weakly correlated to ultimate stress ( $R^2 \sim 0.25$ ) and toughness ( $R^2 \sim 0.24$ ) of cortical bone specimens extracted from the human femur (Granke et al., 2014; Katsamenis et al., 2015) and was correlated ( $R^2 \sim 0.50$ ) with work to failure for pooled data obtained from rat femur, rat vertebra and dog rib (Gallant et al., 2013). Moreover, IDI measurements performed along the longitudinal or transverse directions were found to be similar for the human femoral cortical bone (Granke et al., 2014) but significantly different for porcine cortical bone (Rasouljan et al., 2013). If the relationship between RPI measurements and macro-mechanical properties is not clear, little is known about the relationship between the RPI measurements method and the mechanical properties at the BSU. Surprisingly only two studies (Feng et al., 2012; Rasouljan et al., 2013) compared local lamellar elastic moduli measured with depth sensing nano-indentation (lamellar level, a few microns in size) and RPI measurements on porcine cortical bone, reporting that both techniques measure higher mechanical

properties along the longitudinal direction compared to the transverse one, but it is not clear if indentations were performed on the same set of specimens and along which direction. On the basis of all these studies it appears that there are two crucial factors on which interpretation of the clinical RPI results will depend on in the future: the relationship of RPI measures to the underlying BSUs and the issue of directionality which will determine if and how the application of the RPI locally and *in vivo* will be interpreted as reflecting the properties of the bone at the higher scale.

In this study we propose to investigate the local anisotropic mechanical behaviour of plexiform bone at two dimensional levels with two indentation techniques on the same set of specimens: depth sensing micro-indentation (BSU level, penetration depth equal to 2.5  $\mu\text{m}$ ) and RPI (tissue level, penetration depth approximately 50  $\mu\text{m}$ ).

The hypotheses of this study were that:

- plexiform bone exhibits orthotropic mechanical behaviour at the BSU scale;
- RPI can measure differences in the mechanical properties of the plexiform bone if indented along the axial, radial and circumferential directions;
- there is a relationship between the local mechanical properties measured with RPI and with depth sensing micro-indentation.

## 2. Material and methods

One bovine femur was obtained from an 18 months old animal killed for alimentary purpose. The femur was stored in freezer at  $-20\text{ C}$  until it was dissected.

## 2.1. Specimen preparation and further analysis

Fifteen prismatic specimens ( $3 \times 4 \times 8 \text{ mm}^3$ ) were prepared for indentation tests along the three anatomical directions. In particular, groups of three neighbouring specimens were isolated from five regions of the bone diaphysis. From each group, one sample was prepared for indentation along the axial, one along the radial and one along the circumferential directions. Therefore, five specimens were prepared for indentations along each anatomical direction (Fig. 1c). Specimens were cut with a diamond bandsaw (CP300, Exakt, Germany) under continuous water irrigation to reduce possible damage on the tissue. Afterwards, specimens were left to dehydrate in air for approximately 12 h, then embedded in PMMA (Technovit4071, Heraeus Kulzer, Germany) without infiltration. The specimens were then polished by hand by using progressively finer silicon carbide papers from 400 to 2000 grade (Struers, Denmark) and finalized with alumina paste (0.05  $\mu\text{m}$ , Struers, Denmark). Afterwards, the specimens were rinsed with water in order to remove the polishing particles and left to dehydrate in air for at least 48 h at room temperature. Specimens were visualized under a reflected light microscope and only specimens showing a clear plexiform structure were included in the analysis (Fig. 1d).

For both indentation protocols, measurements were performed on dry specimens in order to minimize the differences between the two measurement techniques.

## 2.2. Micro-indentation test

The specimens were mounted on a calibrated nanoindenter (NHT, CSM-Instruments, Switzerland) and fixed with the upper surface parallel to the horizontal table of the machine. A Berkovich tip was used for the measurements. Twenty-four target indentations were performed for each specimen (in one case only 12 indentations were performed due to surface irregularities). Indentations were performed over an area of  $1000 \times 2100 \mu\text{m}^2$  in order to cover a large portion of the specimen. The target location of the indents was defined based on a virtual rectangular grid, starting at a distance of 1000  $\mu\text{m}$  in both axes from a corner and leaving a distance between each indentations of 300  $\mu\text{m}$  along the X axis and of 500  $\mu\text{m}$  along the Y axes (Fig. 1a). Where necessary the target location of each indentation was corrected in order to avoid measurements on visible defects or macro-pore: once the target position was visualized under the microscope, it was moved within a diameter of 60  $\mu\text{m}$  to avoid surface imperfections or lacunae. In order to avoid edge effects and effects from adjacent indentations, the indentations were performed at least 1000  $\mu\text{m}$  from the edge of the sample, at least 100  $\mu\text{m}$  from each other and at least 100  $\mu\text{m}$  from the vascular pores (Zwierzak et al., 2009). When it was not possible to respect these restrictions, the indentation was skipped.

The indentation procedure consisted in a trapezoidal load-hold-unload procedure in load control, with maximal penetration depth of 2.5  $\mu\text{m}$  and constant loading and unloading rate equal to 120 mN/min (Fig. 1b). In order to minimize the influence of creep, the load at the maximal penetration depth was held for 60 s between loading and unloading linear ramps.

In each indentation the contact point recognized by the machine was corrected by the operator using the standard procedure suggested by the manufacturer. Moreover, curves with unusual shape, due to the presence of defects underneath the surface at the indentation location or due to the requirement of a new depth adjustment, were excluded.

The plane strain indentation modulus ( $E_{\text{ind}}$ , Eqs. (1) and (2)) was calculated according to the Oliver and Pharr (1992). For comparisons with the literature, the elastic modulus ( $E_e$ ) was computed assuming a Poisson's ratio  $\nu_s$  equal to 0.3 (Dall'Ara et al., 2012; Rho et al., 2002; Zioupos, 2005).

$$E_{\text{ind}} = \frac{E_e}{(1 - \nu_s^2)} = \frac{1}{\frac{1}{E_r} - \frac{1 - \nu_s^2}{E_i}} \quad (1)$$

with subscripts indicating bone sample (s) and indenter tip (i);  $E_i$  equal to 1141 GPa and  $\nu_i$  equal to 0.07;  $E_r$  is the reduced indentation modulus and can be computed from the indentation curves as:

$$E_r = \frac{1}{\beta} \frac{\sqrt{\pi}}{2} \frac{1}{\sqrt{A_p(h_c)}} S_{h_{\text{max}}} \quad (2)$$

where  $\beta$  is a constant defined by the shape of the tip,  $S$  is the slope of the unloading curve,  $h_{\text{max}}$  is the maximal depth reached during the indentation,  $A_p$  is the projected area of the indentation at the depth  $h_c$  and it is estimated during the machine calibration test with a fused silica sample.

The aspect ratios between elastic moduli (ARem) were computed from the anisotropy ratios between indentation moduli (ARem = (AR)<sup>1.6</sup>) (Franzoso and Zysset, 2009). Hardness (HV), elastic work  $W_{\text{el}}$  (area below the unloading part of the curve), dissipated work  $W_{\text{pl}}$  (area inscribed by the force–depth cycle) and total work  $W_{\text{tot}}$  (sum of  $W_{\text{el}}$  and  $W_{\text{pl}}$ ) were computed for each indentation (Wolfram et al., 2010).

## 2.3. Reference Point Indentations

Indentations were performed by using the RPI method (BioDent™, Active Life Scientific Inc., USA). As previously described (Jenkins et al., 2015; Setters and Jasiuk, 2014), the instrument performs an indentation on the bone surface with a stainless

steel Bone Probe 2 (BP2; Active Life Scientific) consisting of a 375  $\mu\text{m}$  diameter, cono-spherical, 2.5 mm radius tip probe with a beveled reference probe with a blunted end. The same instrument can be used to perform indentations *in vivo* on (mostly curved) bone surfaces, while here it was used on our standard lab-finished bone specimens to provide comparisons to micro-indentation values. We carried out 10 cycles in load control up to a maximal force of 6 N and with a frequency of 2 Hz (Fig. 1e). The force was increased linearly from zero to maximum load (6 N) during the first one-third of a cycle, maintained for the next one-third and decreased linearly over the final one-third. To be consistent with the micro-indentation experiments, the tests were performed on dry bone, on the micro-indentation-free half of each dry bone specimen (Fig. 1d), leaving 1.0 mm from the edge and 1.4 mm between each indentation (distances larger than the limit of 500  $\mu\text{m}$  suggested by Jenkins et al. (2015)).

For each indentation the following standard parameters were evaluated with the software provided by the manufacturer: the slope of the unloading curve of the first cycle (US1), the mean unloading slope for the 10 cycles (USAvg), the mean dissipated energy in the last seven cycles (EnDisAvg), the mean creep distance in the 10 cycles (CIDAvg), Total Indentation Distance (TID) and the Indentation Distance Increase between first and last cycles (IDI).

In order to check the reliability of the RPI instrument, five indentations were performed on a polished PMMA specimen before and after the tests, at a distance of approximately 2 mm from each other.

## 2.4. Statistics

After exclusion of indentations with unusual indentation graphs, the mean, standard deviations and ranges were calculated for each variable split for “direction” groups (axial, circumferential and radial). As most variables split for “direction” were not normally distributed (Shapiro–Wilk test: 13 variables with  $p < 0.05$ , 23 variables with  $p > 0.05$ , confirmed by the visual inspection of the histograms and of the Q–Q plots), non-parametric tests (Kruskal–Wallis, KW) were performed to test differences for each measurement as a function of the factor “direction”. Linear regressions were performed between the mean values of the RPI and micro-indentation measurement for each specimen by: i) calculating the means of the results obtained for micro-indentation measurements for each specimen ( $E_{\text{ind}}$ , HV,  $W_{\text{pl}}$ ); ii) calculating the means of the values obtained with RPI measurements for each specimen (US1, USAvg, EnDisAvg, IDI); iii) calculating the linear regressions between the RPI and micro-indentation measurements. All analyses were performed using SPSS v20.0 (IBM-Corp, Armonk, NY, USA).

## 3. Results

After the removal of the depth sensing micro-indentations with testing problems (32 indentations), 316 measurements remained valid (117 indentations performed along the axial direction, 107 along the circumferential direction, and 92 along the radial direction). Of the 60 indentations performed with the RPI method, only one was excluded due to contact problems (20 indentations along axial direction, 20 indentations along the radial direction, 19 indentations performed along the circumferential direction). The mean parameters split for “direction” are reported in Table 1.

### 3.1. Depth sensing micro-indentation results

All micro-indentation parameters were dependent on direction ( $p < 0.001$ ) with the exception of  $W_{\text{el}}$  ( $p = 0.436$ ) (Table 1). In particular, the local indentation modulus  $E_{\text{ind}}$  was found to be highest for the axial direction ( $24.3 \pm 2.5$  GPa) compared to the one from circumferential indentations (19% less stiff) and from the radial direction (30% less stiff). ARem were 1.41 and 1.79 for axial/circumferential (ARem-ac) and axial/radial (ARem-ar) directions, respectively. Similar trends were found for the hardness ( $70.6 \pm 7.2$  kg/mm<sup>2</sup> for the axial direction, 13% less hard for circumferential direction, 21% less hard for radial direction), for the dissipated work  $W_{\text{pl}}$  ( $0.084 \pm 0.011$   $\mu\text{J}$  for axial, 20% lower for circumferential and 27% lower for radial directions) and for the total Work ( $W_{\text{tot}} = 0.110 \pm 0.015$   $\mu\text{J}$  for axial, 14% lower for circumferential and 20% lower for radial directions). For pooled data, weak to moderate relationships were found between  $E_{\text{ind}}$  and HV ( $p < 0.001$ ,  $R^2 = 0.64$ ),  $W_{\text{pl}}$  ( $p < 0.001$ ,  $R^2 = 0.72$ ) and  $W_{\text{tot}}$  ( $p < 0.001$ ,  $R^2 = 0.56$ ), but no correlation was found with  $W_{\text{el}}$  ( $p = 0.820$ ) (Fig. 2). When split for “direction”, significant correlations between  $E_{\text{ind}}$  and the



**Table 1**  
Results (mean  $\pm$  SD) from the micro-indentation and the RPI tests reported for different indentation directions. On the right column the  $p$ -value for the KW tests are reported.

		Axial	Circumferential	Radial	KW
<b>Micro-indentation</b>	$E_{ind}$ [GPa]	24.3 $\pm$ 2.5	19.6 $\pm$ 3.1	16.9 $\pm$ 1.4	$p < 0.001$
	HV [kg/mm <sup>2</sup> ]	70.6 $\pm$ 7.2	61.6 $\pm$ 7.3	55.6 $\pm$ 6.2	$p < 0.001$
	$W_{el}$ [ $\mu$ J]	0.027 $\pm$ 0.005	0.027 $\pm$ 0.003	0.027 $\pm$ 0.004	$p = 0.436$
	$W_{pl}$ [ $\mu$ J]	0.084 $\pm$ 0.011	0.067 $\pm$ 0.010	0.061 $\pm$ 0.006	$p < 0.001$
	$W_{tot}$ [ $\mu$ J]	0.110 $\pm$ 0.015	0.095 $\pm$ 0.011	0.088 $\pm$ 0.008	$p < 0.001$
<b>RPI-BioDent</b>	US1 [N/ $\mu$ m]	0.47 $\pm$ 0.03	0.42 $\pm$ 0.03	0.39 $\pm$ 0.03	$p < 0.001$
	USAvg [N/ $\mu$ m]	0.48 $\pm$ 0.03	0.43 $\pm$ 0.03	0.40 $\pm$ 0.03	$p < 0.001$
	IDI [ $\mu$ m]	4.6 $\pm$ 0.3	4.8 $\pm$ 0.5	4.8 $\pm$ 0.5	$p = 0.173$
	EnDisAvg [ $\mu$ J]	12.0 $\pm$ 1.6	14.2 $\pm$ 1.7	14.9 $\pm$ 1.5	$p < 0.001$
	TID [ $\mu$ m]	49.8 $\pm$ 2.5	51.0 $\pm$ 2.0	51.8 $\pm$ 1.7	$p < 0.001$
	CIDAvg [ $\mu$ m]	0.9 $\pm$ 0.1	1.1 $\pm$ 0.1	1.1 $\pm$ 0.11	$p < 0.001$

other indentation properties were found for the circumferential direction ( $R^2 = 0.59$  for HV,  $R^2 = 0.73$  for  $W_{pl}$  and  $R^2 = 0.57$  for  $W_{tot}$ ;  $p < 0.001$  for all of them), while weak, albeit significant ( $p < 0.001$ ), correlations were found for the other directions ( $R^2 = 0.16$  and  $R^2 = 0.33$  for the radial and axial directions only) (Fig. 2).

### 3.2. RPI results

The results from the indentations on the PMMA showed small differences between the pre- and post-tests on bone: absolute value of the difference between the means from 0.68% (USAvg) to 3.96% (EnDisAvg), differences in the coefficient of variations from 0.65% (EnDisAvg) to 4.86% (CIDAvg).

All RPI measurements on plexiform bone were found to be dependent on indentation direction ( $p < 0.001$ ) with the exception of IDI ( $p = 0.173$ ) (Table 1). In particular, US1 was found to be greater for axial oriented specimens (0.47  $\pm$  0.03 N/ $\mu$ m) compared to circumferential (11% lower) and radial ones (17% lower). Similar trends were found for USAvg (0.48  $\pm$  0.03 N/ $\mu$ m for axial, 10% lower for circumferential and 17% lower for radial specimens). Opposite trends were found for CIDAvg (0.9  $\pm$  0.1  $\mu$ m for axial, 11% higher for circumferential and 18% higher for radial specimens) and TID (49.8  $\pm$  2.5  $\mu$ m for axial, 2% higher for circumferential and 4% higher for radial specimens). It must be noted that IDI was not found to depend on direction even if results were split into axial and transverse groups (with radial and circumferential directions pooled in one group;  $p = 0.076$ , IDI transverse equal to 4.8  $\pm$  0.5  $\mu$ m, difference of 4.5%).

### 3.3. Comparison between micro-indentation and RPI

Comparison between the mean values of the micro-indentation and RPI measurements for the same specimens are reported in Fig. 3. Significant but moderate positive correlations were found between US1 and  $E_{ind}$  ( $p = 0.001$ ;  $R^2 = 0.58$ ) and between US10 and  $E_{ind}$  ( $p = 0.001$ ;  $R^2 = 0.54$ ). Conversely, significant but moderate negative correlations were found between  $W_{pl}$  and EnDisAvg ( $p = 0.007$ ;  $R^2 = 0.44$ ) and between EnDisAvg and HV ( $p = 0.007$ ,  $R^2 = 0.44$ ). Furthermore, no significant relationship was found between IDI and either  $E_{ind}$  ( $p = 0.157$ ) or HV ( $p = 0.197$ ).

## 4. Discussion

The aim of this study was to investigate if the RPI approach is able to discriminate the anisotropic properties of plexiform bone, in comparison with a well-established technique such as depth sensing micro-indentation.

The micro-indentation tests confirmed the hypothesis that plexiform bone is orthotropic also at the tissue level. The  $E_{ind}$  of BSU tested along the longitudinal direction for bovine plexiform bone

(24.3  $\pm$  2.5 GPa) was similar to the values reported for the human tibia (24.7–28.4 GPa, (Rho et al., 1997)) but higher than for the human cortical shell (14.5  $\pm$  2.5 GPa (Dall'Ara et al., 2013) and 19.9  $\pm$  2.7 GPa (Roy et al., 1999)). The anisotropy ratios measured for of plexiform bone were different than the values reported for human cortical shell (ARem-ac equal to 1.41 vs 1.32 (Dall'Ara et al., 2013) and 1.11 (Roy et al., 1999); ARem-ar equal to 1.79 vs 2.47 (Dall'Ara et al., 2013)). These differences may arise from lamellar arrangement and local heterogeneity in mineral density. More analyses are required to clarify which tissue properties contribute significantly to local anisotropy. Moreover, we found ARem at the BSU level in line with the those reported from ultrasound measurements performed on human and canine bone tissue (Turner et al., 1995, 1999) and those measured at the macro-level on bovine plexiform bone (Katz et al., 1984; Macione et al., 2010). The differences in  $E_{ind}$ , HV and  $W_{pl}$  along the different directions may suggest that the microstructure of the plexiform bone has intrinsic differences in both the mineral phase, which is related to the elastic deformation, and collagen composition and orientation, which is related to the plastic deformation (Bala et al., 2011). The overall correlation between  $E_{ind}$  and HV or  $W_{pl}$  for pooled data and for circumferential direction may be related to an underlying relationship between the amount of mineral and the plastic deformation effects in this type of tissue.

The measurements performed at the tissue level on flat polished bone surfaces with the RPI method showed dependence on the specimen orientation in all parameters, except for IDI. This result is consistent with previous reports on bovine bone (Jenkins et al., 2015) and on human femoral specimens (Granke et al., 2014), but is in contrast with data on porcine femurs (Rasouljan et al., 2013) where lower IDI values were found for longitudinal indentations compared to transverse ones. These differences might arise from species or age related factors. It remains to be investigated why IDI is not a systematically related to the indentation direction for the different studies. Considering that the RPI technique is currently the solely technique used for material characterization *in vivo*, the present data stresses that the IDI along the radial direction (suggested output for clinical applications) cannot be used to predict the IDI along the other directions. While this may seem to be a drawback, it is also a “benefit in disguise”. In clinical applications, where the exposed bone surface is almost invariably ill-defined in terms of direction and certainly never flat, the independency of IDI from the indentation direction may be an advantage. In fact, it allows intergroup properties to be revealed such as comparisons between healthy and osteoporotic patients, without the need to specifying directional differences. The practicality good use of IDI in clinical applications may in fact owe a lot to this simple “accidental” fact. It remains to be investigated whether similar results would be obtained in preclinical or clinical conditions where measurements are performed on the periosteum of a curved un-embedded wet bone surface.

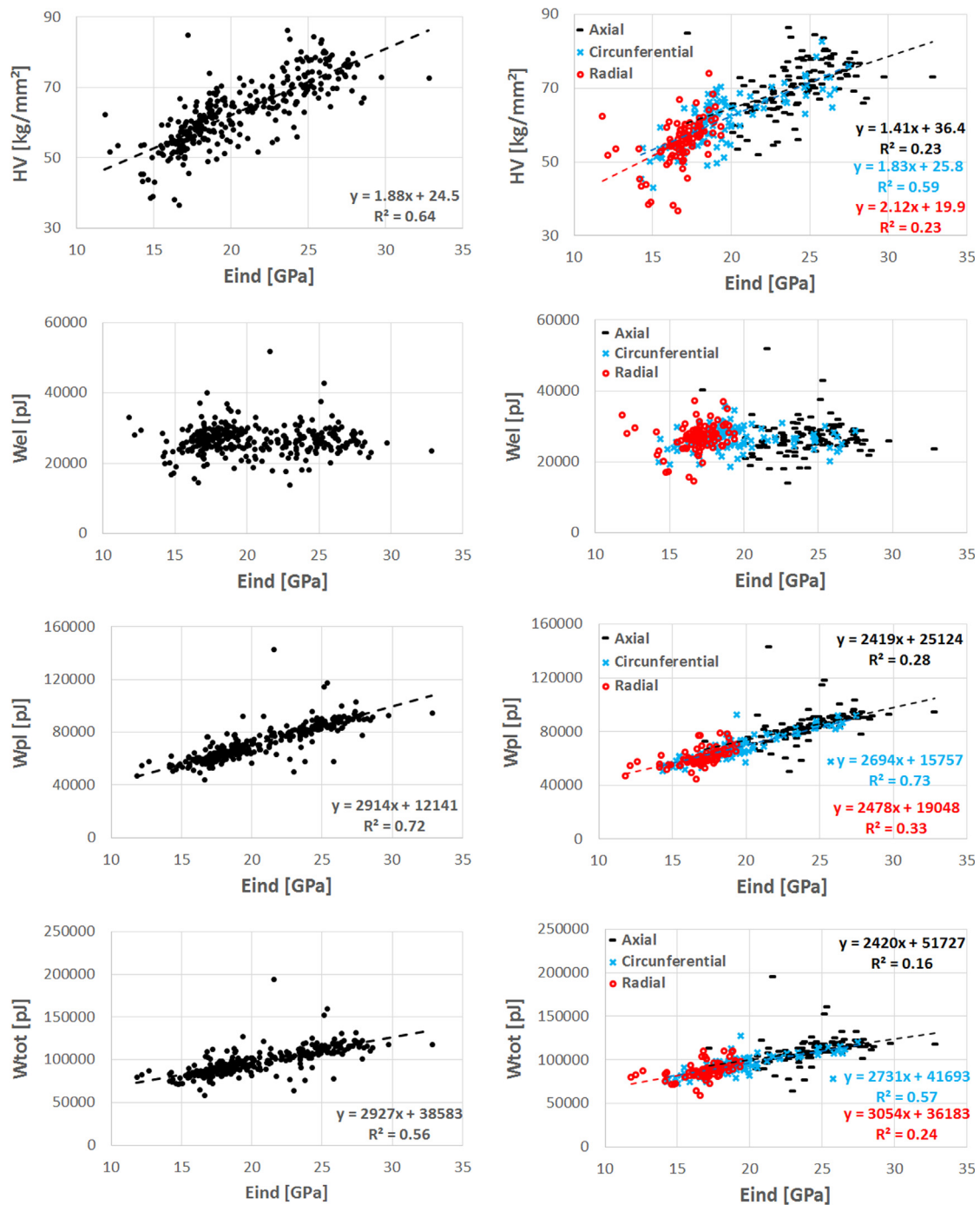


**Fig. 2.** Results from micro-indentation tests. Linear regression analysis among the micro-indentation measurements (indentation modulus  $E_{ind}$ , hardness HV, elastic work  $W_{el}$ , and dissipated work  $W_{pl}$ ) for pooled data (left) and for data split for indentation directions (right). Equations and regression lines were reported when significant correlations were found.

This is the first study to report the relationship between RPI and micro-indentation measurements performed on the same set of specimens and along different anatomical directions. The results showed a moderate positive correlation between the micro-indentation  $E_{ind}$  and US1 ( $R^2=0.58$ ) or US10 ( $R^2=0.54$ ). In fact, RPI measurements, undertaken with deeper penetration, are affected by the properties of a larger bone volume under the tip, which is composed of different microarchitectures that affect the local material properties (Oyen and Ko, 2008; Paietta et al., 2011). Furthermore, the differences between the mechanical properties measured with the two methods could also be due to the different tip used (Berkovich vs conico-spherical) (Olesiak et al., 2010) and

the indentation rate. Even though these results could be specific to plexiform bone, we have shown that RPI measurements (100  $\mu\text{m}$  scale) explain 44–58% of the variations in indentation modulus measured with depth sensing micro-indentation (1–10  $\mu\text{m}$  scale). Further work should be done to test if these results could be extended for osteonal bone. Contrasting results were reported in the literature about the relationship between the RPI outputs and measurements performed at the 1000–10,000  $\mu\text{m}$  scale showing no correlation (Carriero et al., 2014) or weak-moderate correlations (Gallant et al., 2013; Granke et al., 2014; Katsamenis et al., 2015) with bone toughness. The data suggests that the relationships may be dependent on the type of bone studied, ranging from

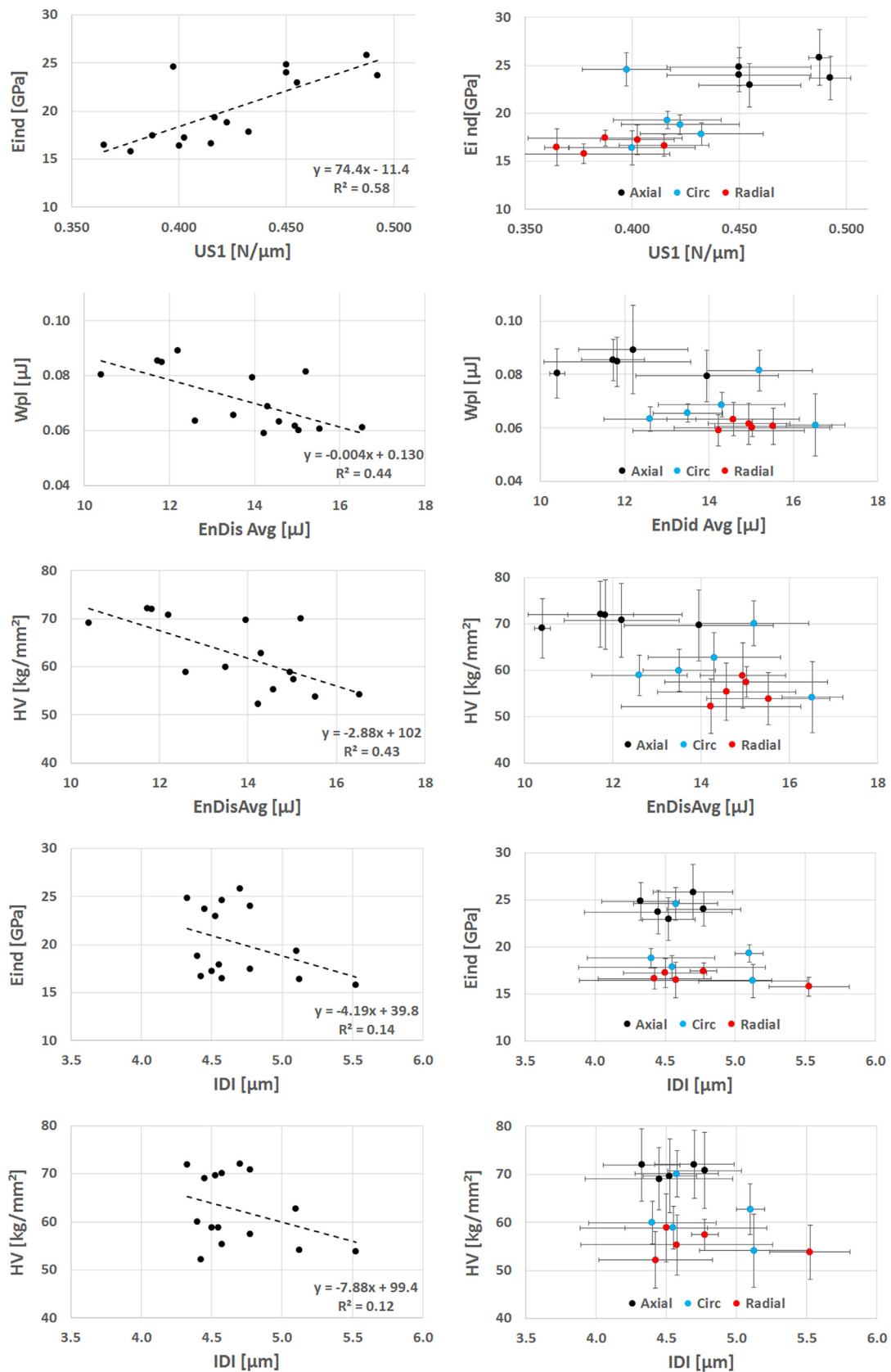


**Fig. 3.** Comparison between micro-indentation and RPI measurements. Correlations among the mean values of RPI (slope of the unloading curve of the first cycle US1, average dissipated energy in the last seven cycles EnDisAvg, and Indentation Distance Increase IDI) and micro-indentation (indentation modulus  $E_{ind}$ , hardness HV, and dissipated work  $W_{pl}$ ) measurements reported for each sample. On the left column measurements have been pooled for all indentation directions with linear regression equations and coefficients of determination. On the right measurements are split for indentation direction and reported with the standard deviations for both measurements type (error bars).

mice to human bones. In the relationships between RPI and micro-indentation data, it seems that one specimen is an outlier. However, because no reason for its behaviour could be found, the results in this study have been reported including all specimens. Yet, in case that specimen would be excluded, most of the correlations improved ( $E_{\text{ind}}\text{-US1}$  from  $R^2=0.58$  to  $R^2=0.79$ ;  $E_{\text{ind}}\text{-US10}$  from  $R^2=0.54$  to  $R^2=0.77$ ;  $W_{\text{pl}}\text{-EnDisAvg}$  from  $R^2=0.44$  to  $R^2=0.59$ ;  $HV\text{-EnDisAvg}$  from  $R^2=0.44$  to  $R^2=0.61$ ). However, yet again no improvement was found for the correlations with IDI, for which the relationships remained almost identical ( $E_{\text{ind}}\text{-IDI}$  from  $R^2=0.14$  to  $R^2=0.13$  and  $HV\text{-IDI}$  from  $R^2=0.12$  to  $R^2=0.12$ ).

There are some limitations within the present study. Indentations were performed under dry conditions. Although dehydration affects the absolute values measured by micro-indentation, it has no effect as far as patterns of behaviour are concerned (*i.e.* directional effects, mineralization levels *etc.*) other than shifting the base line of the data higher by 10–20% (Wolfram et al., 2010). However, it is possible that the dehydration could have different impact on the measurement performed at the two dimensional levels with potential influence on the results. Another limitation is the use of only one animal (bovine), one anatomical site (femur) and one bone tissue (plexiform). It remains to be investigated whether similar conclusions would be valid for other types of bone tissue (*e.g.* osteonal bone), species (*e.g.* human and porcine) and anatomical sites (*e.g.* vertebra). The design of these other experiments, of course, will have to be informed by the need for use of RPI in various other relevant clinical scenarios. Finally, only four RPI indentations were performed on each sample.

The main conclusions of this study can be summarized as follows:

- depth sensing micro-indentation can discriminate the orthotropic mechanical properties of plexiform bone at the BSU level;
- under the studied conditions, most of the RPI measurements can also measure differences in the mechanical properties of the tissue in different directions, with the noted exception of IDI, the most commonly quoted parameter for *in vivo* clinical applications;
- there is a linear relationship between most local mechanical properties measured with RPI and those measured locally with micro-indentations. However, no relationship was found between IDI and either of the micro-indentation parameters  $E_{\text{ind}}$  or HV.

Finally, we found for the first time that there is a better relationship between the RPI outputs (apart from IDI) and mechanical properties at the BSU compared to those measured at the macro-architectural scale (toughness of whole mice bones or of cortical bone specimens in the range of a few millimetres) reported in the literature. In addition the IDI has limitations in estimating the axial and circumferential mechanical properties of cortical bone from measurements performed *in vivo* along the radial direction. This result means that the applicability of the IDI method is restricted to projects where the estimation of the local anisotropy is not important. However, this may be advantageous when directionality is ill-defined or irrelevant and differences between group data are required. In these cases directionality can be ignored as a factor.

#### Conflict of interest statement

The authors have no conflict of interest for this study.

#### Acknowledgements

The project was partially funded by the FP7 European Program (MAMBO: PIEF-GA-2012-327357) and EPSRC MultiSim project (EP/

K03877X/1). PZ would like to acknowledge the support of EPSRC (EP/K020196: Point-of-Care High Accuracy Fracture Risk Prediction) research grant. The authors would like to thank Mr Podgorski for the help with the specimen preparation and Professor Bishop for access to the Biodent.

#### References

- Bala, Y., Depalle, B., Douillard, T., Meille, S., Clement, P., Follet, H., Chevalier, J., Boivin, G., 2011. Respective roles of organic and mineral components of human cortical bone matrix in micromechanical behavior: an instrumented indentation study. *J. Mech. Behav. Biomed. Mater.* 4, 1473–1482.
- Carriero, A., Bruse, J.L., Oldknow, K.J., Millan, J.L., Farquharson, C., Shefelbine, S.J., 2014. Reference point indentation is not indicative of whole mouse bone measures of stress intensity fracture toughness. *Bone* 69, 174–179.
- Dall'Ara, E., Karl, C., Mazza, G., Franzoso, G., Vena, P., Pretterklieber, M., Pahr, D., Zysset, P., 2013. Tissue properties of the human vertebral body sub-structures evaluated by means of microindentation. *J. Mech. Behav. Biomed. Mater.* 25, 23–32.
- Dall'Ara, E., Schmidt, R., Zysset, P., 2012. Microindentation can discriminate between damaged and intact human bone tissue. *Bone* 50, 925–929, Epub 2012 Jan 2014.
- Diez-Perez, A., Guerri, R., Nogues, X., Caceres, E., Pena, M.J., Mellibovsky, L., Randall, C., Bridges, D., Weaver, J.C., Proctor, A., Brimer, D., Koester, K.J., Ritchie, R.O., Hansma, P.K., 2010. Microindentation for *in vivo* measurement of bone tissue mechanical properties in humans. *J. Bone Miner. Res.* 25, 1877–1885.
- Feng, L., Chittenden, M., Schirer, J., Dickinson, M., Jasiuk, I., 2012. Mechanical properties of porcine femoral cortical bone measured by nanoindentation. *J. Biomech.* 45, 1775–1782.
- Franzoso, G., Zysset, P.K., 2009. Elastic anisotropy of human cortical bone secondary osteons measured by nanoindentation. *J. Biomech. Eng.* 131, 021001.
- Gallant, M.A., Brown, D.M., Organ, J.M., Allen, M.R., Burr, D.B., 2013. Reference-point indentation correlates with bone toughness assessed using whole-bone traditional mechanical testing. *Bone* 53, 301–305.
- Granke, M., Coulmier, A., Uppuganti, S., Gaddy, J.A., Does, M.D., Nyman, J.S., 2014. Insights into reference point indentation involving human cortical bone: sensitivity to tissue anisotropy and mechanical behavior. *J. Mech. Behav. Biomed. Mater.* 37, 174–185.
- Guerri-Fernandez, R.C., Nogues, X., Quesada Gomez, J.M., Torres Del Pliego, E., Puig, L., Garcia-Giral, N., Yoskovitz, G., Mellibovsky, L., Hansma, P.K., Diez-Perez, A., 2013. Microindentation for *in vivo* measurement of bone tissue material properties in atypical femoral fracture patients and controls. *J. Bone Miner. Res.* 28, 162–168.
- Hansma, P., Turner, P., Drake, B., Yurtsev, E., Proctor, A., Mathews, P., Lulejian, J., Randall, C., Adams, J., Jungmann, R., Garza-de-Leon, F., Fantner, G., Mkrtchyan, H., Pontin, M., Weaver, A., Brown, M.B., Sahar, N., Rossello, R., Kohn, D., 2008. The bone diagnostic instrument II: indentation distance increase. *Rev. Sci. Instrum.* 79, 064303.
- Hansma, P., Yu, H., Schultz, D., Rodriguez, A., Yurtsev, E.A., Orr, J., Tang, S., Miller, J., Wallace, J., Zok, F., Li, C., Souza, R., Proctor, A., Brimer, D., Nogues-Solan, X., Mellibovsky, L., Pena, M.J., Diez-Ferrer, O., Mathews, P., Randall, C., Kuo, A., Chen, C., Peters, M., Kohn, D., Buckley, J., Li, X., Pruitt, L., Diez-Perez, A., Alliston, T., Weaver, V., Lotz, J., 2009. The tissue diagnostic instrument. *Rev. Sci. Instrum.* 80, 054303.
- Jenkins, T., Coutts, L.V., Dunlop, D.G., Oreffo, R.O., Cooper, C., Harvey, N.C., Thurner, P.J., 2015. Variability in reference point microindentation and recommendations for testing cortical bone: maximum load, sample orientation, mode of use, sample preparation and measurement spacing. *J. Mech. Behav. Biomed. Mater.* 42, 311–324.
- Katsamenis, O.L., Jenkins, T., Thurner, P.J., 2015. Toughness and damage susceptibility in human cortical bone is proportional to mechanical inhomogeneity at the osteonal-level. *Bone* 76, 158–168.
- Katz, J.L., Yoon, H.S., Lipson, S., Maharidge, R., Meunier, A., Christel, P., 1984. The effects of remodeling on the elastic properties of bone. *Calcif. Tissue Int.* 36 (Suppl 1), S31–S36.
- Li, S., Demirci, E., Silberschmidt, V.V., 2013. Variability and anisotropy of mechanical behavior of cortical bone in tension and compression. *J. Mech. Behav. Biomed. Materials.* 21, 109–120.
- Macione, J., Depaula, C.A., Guzelsu, N., Kotha, S.P., 2010. Correlation between longitudinal, circumferential, and radial moduli in cortical bone: effect of mineral content. *J. Mech. Behav. Biomed. Mater.* 3, 405–413.
- Odgaard, A., 1997. Three-dimensional methods for quantification of cancellous bone architecture. *Bone* 20, 315–328.
- Ohman, C., Baleani, M., Perilli, E., Dall'Ara, E., Tassani, S., Baruffaldi, F., Viceconti, M., 2007. Mechanical testing of cancellous bone from the femoral head: experimental errors due to off-axis measurements. *J. Biomech.* 40, 2426–2433.
- Olesiak, S.E., Oyen, M.L., Ferguson, V.L., 2010. Viscous-elastic-plastic behavior of bone using Berkovich nanoindentation. *Mech. Time-Depend. Mater.* 14, 111–124.
- Oliver, W.C., Pharr, G.M., 1992. An improved technique to determine hardness and elastic modulus using load and displacement sensing indentation experiments. *J. Mater. Res.* 7, 1564–1583.
- Oyen, M.L., Ko, C.C., 2008. Indentation variability of natural nanocomposite materials. *J. Mater. Res.* 23, 760–767.

- Paietta, R.C., Campbell, S.E., Ferguson, V.L., 2011. Influences of spherical tip radius, contact depth, and contact area on nanoindentation properties of bone. *J. Biomech.* 44, 285–290.
- Rasoulian, R., Raeisi Najafi, A., Chittenden, M., Jasiuk, I., 2013. Reference point indentation study of age-related changes in porcine femoral cortical bone. *J. Biomech.* 46, 1689–1696.
- Reisinger, A.G., Pahr, D.H., Zysset, P.K., 2011. Elastic anisotropy of bone lamellae as a function of fibril orientation pattern. *Biomech. Model. Mechanobiol.* 10, 67–77, Epub 2010 Apr 2027.
- Rho, J.Y., Tsui, T.Y., Pharr, G.M., 1997. Elastic properties of human cortical and trabecular lamellar bone measured by nanoindentation. *Biomaterials* 18, 1325–1330.
- Rho, J.Y., Zioupos, P., Currey, J.D., Pharr, G.M., 2002. Microstructural elasticity and regional heterogeneity in human femoral bone of various ages examined by nano-indentation. *J. Biomech.* 35, 189–198.
- Rincon-Kohli, L., Zysset, P.K., 2009. Multi-axial mechanical properties of human trabecular bone. *Biomech. Model. Mechanobiol.* 8, 195–208.
- Roy, M.E., Rho, J.Y., Tsui, T.Y., Evans, N.D., Pharr, G.M., 1999. Mechanical and morphological variation of the human lumbar vertebral cortical and trabecular bone. *J. Biomed. Mater. Res.* 44, 191–197.
- Setters, A., Jasiuk, I., 2014. Towards a standardized reference point indentation testing procedure. *J. Mech. Behav. Biomed. Mater.* 34, 57–65.
- Turner, C.H., Chandran, A., Pidaparti, R.M., 1995. The anisotropy of osteonal bone and its ultrastructural implications. *Bone* 17, 85–89.
- Turner, C.H., Rho, J., Takano, Y., Tsui, T.Y., Pharr, G.M., 1999. The elastic properties of trabecular and cortical bone tissues are similar: results from two microscopic measurement techniques. *J. Biomech.* 32, 437–441.
- Wolfram, U., Wilke, H.J., Zysset, P.K., 2010. Rehydration of vertebral trabecular bone: influences on its anisotropy, its stiffness and the indentation work with a view to age, gender and vertebral level. *Bone* 46, 348–354.
- Zioupos, P., 2005. In vivo fatigue microcracks in human bone: material properties of the surrounding bone matrix. *Eur. J. Morphol.* 42, 31–41.
- Zwierzak, I., Baleani, M., Viceconti, M., 2009. Microindentation on cortical human bone: effects of tissue condition and indentation location on hardness values. *Proc. Inst. Mech. Eng. Part H: J. Eng. Med.* 223, 913–918.